

A Molding Surface Auto-Inspection System

Ssu-Han Chen, Der-Baau Perng

Abstract—Molding process in IC manufacturing secures chips against the harms done by hot, moisture or other external forces. While a chip was being molded, defects like cracks, dilapidation, or voids may be embedding on the molding surface. The molding surfaces the study poises to treat and the ones on the market, though, differ in the surface where texture similar to defects is everywhere. Manual inspection usually passes over low-contrast cracks or voids; hence an automatic optical inspection system for molding surface is necessary. The proposed system is consisted of a CCD, a coaxial light, a back light as well as a motion control unit. Based on the property of statistical textures of the molding surface, a series of digital image processing and classification procedure is carried out. After training of the parameter associated with above algorithm, result of the experiment suggests that the accuracy rate is up to 93.75%, contributing to the inspection quality of IC molding surface.

Keywords—Molding surface, machine vision, statistical texture, discrete Fourier transformation.

I. INTRODUCTION

MOLDING is one of steps of packaging procedure of IC, which starts by setting and pre-heating welded lead frame or substrate onto the framework. Then, the framework is installed on packaging module of the mold press, with half-melted resin squeezed in it. The molding task is finished after the filling process is done and the resin is hardened. The quality of molding determines the success of the product, and the outlook, function of the artifact as well. However, defects occur due to the aberration of parameter configuration and unexpected procedural instability. Defects include cracks, dilapidation and voids. Among them, dilapidation could be more easily detectable during human inspection, whereas a very tiny crack and void are often neglected. To improve the quality of the IC manufacturing, the importance of developing a set of automatic optical inspection system for IC molding surface cannot be neglected.

Previously contactless inspection system for IC molding surface resorted to the scanning acoustic microscopy (SAM), which is sensitive to defects on the contact area [1]. The system could detect and locate defects of plastic IC with C-type SAM. Ong, Tan, and Tan used the C-type to locate molding void and also the B-type to measure its depth [2]. Ma, Bao, Lv, Du, and Li conducted comparative analysis of defect inspection results of plastic IC derived from A-, B-, C- and T-type SAMs. The experiment found that the C-type's scanning way of

cross-sectional view is the most efficient [3]. The automatic optical inspection system for IC molding surface is rarely introduced may be that the procedure of the surface to be inspected is less complicated. The molding body is dark-colored and its defect more conspicuous, hence defects would be displayed by simple binarization image processing method. It goes without saying a system like that is commercially lucrative. The moldings the study poises to treat and the ones on the market, however, differ in the surface where texture similar to imperfections is everywhere. As a result, for our research the goal of defect inspection cannot be achieved in facile ways as mentioned above.

The research develops a solution of automatic optical inspection system for IC molding surface based on machine vision. The proposed system is an image-capturing optical module composed of a CCD, a coaxial light and a back light, namely a set of high magnification microscope altogether. An X-Y motion control unit is adopted to photograph the molding surface. In addition, the snapshot is restored by discrete Fourier transformation (DFT) scheme, coupled with statistical control charts, binarization process and feature extraction to highlight the defects.

II. RESEARCH METHODS

A. Hardware Configuration

Fig. 1 refers to the prototype of hardware framework developed by in this research concerning the proposed automatic optical system to inspect the defects embedded on IC molding surface. The units primarily comprise an image-captured module and an X-Y motion control platform. The image-retrieval machinery includes a CCD, a coaxial light and a back light module. Confined by the specular reflection from the molding surface, the research irradiates the fully front molding with red LED coaxial light, generating bright and tender light field on the area to be inspected. This practice eliminates shadow caused by the uneven surface and rids the image of undesirable reflection, glare and other interference. To erase the noises encircling the molding, the study introduces a white back light and lets it go through the dark gray circles. An acrylic plate is inserted between the object being inspected and the back light to soften the light field.

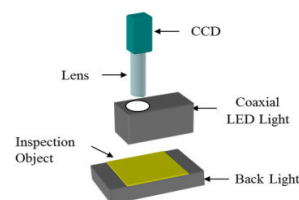


Fig. 1 Automatic optical inspection system for IC molding surface

Ssu-Han Chen is with the Department of Industrial Engineering and Management, Ming Chi University of Technology, New Taipei City, 24301, Taiwan (phone: 886-2-2908-9899#3104; fax: 886-2-29085900; e-mail: ssuhanchen@mail.mcut.edu.tw).

Der-Baau Perng is with the Department of Applied Informatics and Multimedia, Department of International Business, Asia University, Taichung, Taiwan (e-mail: perng@asia.edu.tw).

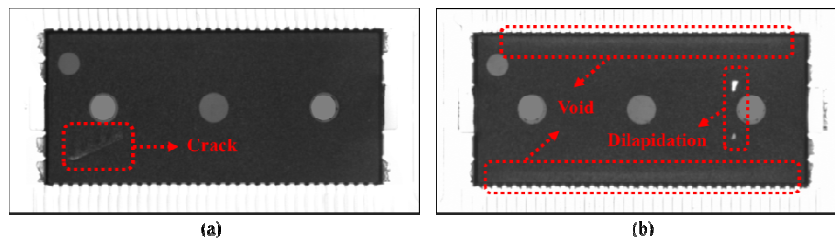


Fig. 2 Types of defects on molding surface

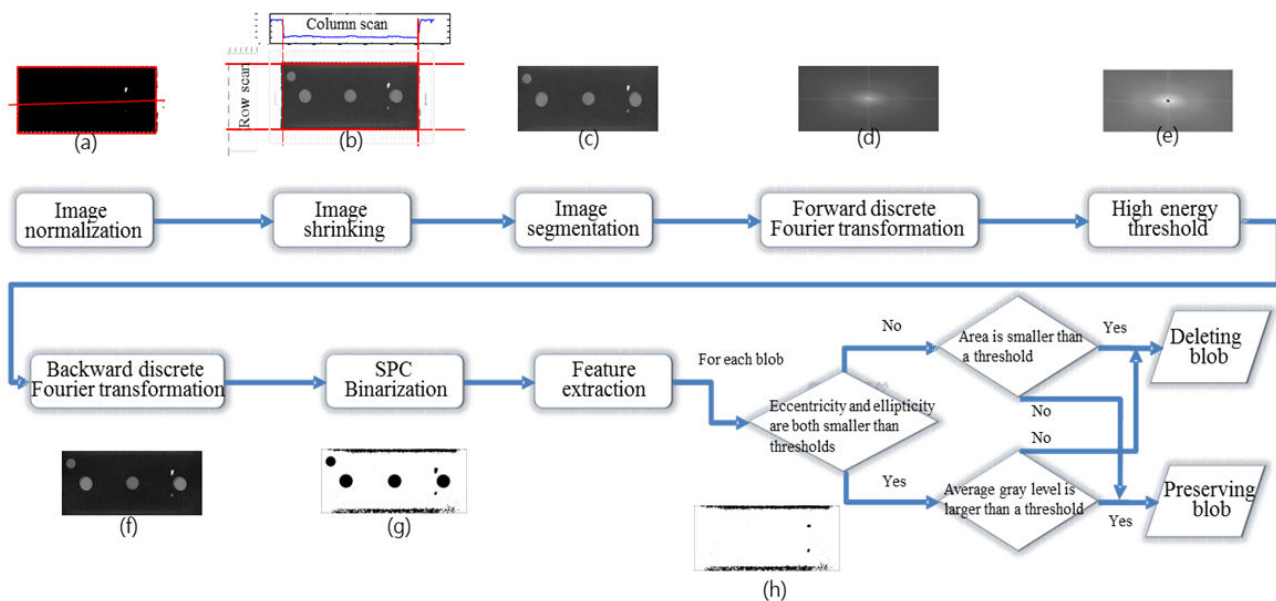


Fig. 3 Flow chart of defect inspection algorithm

In Fig. 2 we can see a slightly white area surrounding the molding, a dark rectangle with one smaller and three bigger circles. Randomly, densely scattered on the molding surface is statistical texture whose brightness and shape are close to the circles', which plays a pivotal role in the experiment. Cracks, voids and dilapidation are indicated in Fig. 2 other than the texture.

B. Defect Inspection Algorithm

To automatically detect the defects attached on the molding surface with statistical texture, the research develops an inspection algorithm, covering three sub-functions: normalization of images, shrinking and segmenting, Fourier-based image restoration scheme and defect identification. The algorithm is described explicitly as following, and the flow chart is introduced in Fig. 3.

1. Image Normalization, Shrinking and Segmenting

The black molding surface is the ROI of the research. In Section II A we have described the image-captured module shown as Fig. 1. The module contrasts the molding and its peripheral metal frames, which makes segmenting of molding easier. Take Fig. 2 (b) for instance, we use Otsu thresholding to capture automatically the molding area which has lower gray values. Then, from its bounding rectangular angle, the image

can be rotated with affine transformation indicated as presented by Fig. 3 (a).

The normalization is followed by calculation of average gray value of each row and column respectively. As the two line charts in Fig. 3 (b) have suggested, the average gray value drops off abruptly during the scanning process, i.e. from brightness to darkness. Typically, the central axis of the dark rectangular molding surface is characterized by the line lingering at the bottom. The coordinate axis could be estimated by the minimum of the first or third quartile of the average gray value. Fig. 3 (c) best shows the result of the image segmenting; just the black molding body is kept, and the bordering frames are discarded.

2. Discrete Fourier-Based Image Restoration Scheme

In order to make defects prominent in the molding image constituted by statistical texture, the research adopts the discrete Fourier-based image restoration scheme [4], blurring the texture of the molding. The identical scheme is also applied to images with directional texture [5]. The approach is based upon image restoration procedure in the frequency domain, where feature identification is needless. Comparison with reference images is not necessary, neither. Its advantage is two-folded: first, the feature selection problem of partial feature

extraction method is shunned; second, calibration problem of golden template matching method is eliminated. That is why so much attention is paid to the global approach.

To start with, transform Fig. 3 (c) into the frequency domain through forward DFT denoted by (1)

$$F(u, v) = \frac{1}{mn} \sum_{x=0}^{m-1} \sum_{y=0}^{n-1} f(x, y) e^{-2j\pi(ux/m+vy/n)} \quad (1)$$

where $f(x, y)$ represents the gray value of the pixel located at coordinate (x, y) in the image waiting to be inspected. Besides, map the $F(u, v)$ with larger dynamic range onto $P(u, v)$

$$P(u, v) = S[\log(1 + |F(u, v)|)] \quad (2)$$

where $S(\cdot)$ corresponds to the scaling operator, and $|\cdot|$ the absolute value operator. As Fig. 3 (d) has expressed, together with the circular pattern, the molding texture has been transformed into the frequency domain from the spatial domain.

To blur the statistical texture in the spatial domain, we can use the notch-rejected filters in the frequency domain, represented by (3), and filter out the high-energy items delegating the texture of molding surface. As far as the study has observed, the high-energy items of statistical texture are concentrated around the center of the image in the frequency domain. After using the notch-rejected filters, we collect an image in the frequency domain, shown in Fig. 3 (e)

$$F(u, v) = \begin{cases} 0 & , \text{if } P(u, v) \geq k1 \\ F(u, v) & , \text{o.w.} \end{cases} \quad (3)$$

where $k1 \in [0, 1]$, serves as the high-energy threshold, aiming at the removal of statistical texture for one thing and the reservation of the circular pattern for another thing. The goal cannot be achieved without the training of parameter sensitivity analysis.

Moreover, transform Fig. 3 (e) back into the spatial domain through backward DFT denoted by (4). The result, so-called restored image, is exhibited by Fig. 3 (f).

$$\hat{f}(x, y) = \frac{1}{mn} \sum_{u=0}^{m-1} \sum_{v=0}^{n-1} F(u, v) e^{2j\pi(ux/m+vy/n)} \quad (4)$$

Besides, according to Fig. 3 (f), the random molding texture has become fuzzy, of which the gray values are evenly curbed. In contrast, the gray values of the brighter defects and circulars are kept.

At last, in the light of statistical process control binarization method denoted by (5), the research restores the brighter defects and circular patterns existed in the image and establishes upper control limit (UCL)

$$\hat{f}(x, y) = \begin{cases} 1 & , \text{if } \hat{f}(x, y) < \mu_{\hat{f}} + k2 \cdot \sigma_{\hat{f}} \\ 0 & , \text{o.w.} \end{cases} \quad (5)$$

where $k2$ is the control constant; $\mu_{\hat{f}}$ and $\sigma_{\hat{f}}$ represents the mean and standard deviation of the gray value of the restored image. On one hand, as Fig. 3 (g) has expressed, pixels of the restored image are white-colored if they fall inside the limit, meaning that they ought to be deleted. On the other hand, the black-colored pixels are what need to be kept, including the defects and circular patterns.

3. Defect Identification

In a binary image, the circular patterns or defects, if any, coexist; but they should be distinct. Features of each connected item could be extracted thanks to the binary large object (blob) analysis. Next, the circular patterns and defects are discriminated through thresholding. Thus the gray values of pixels belonging to the circular patterns in Fig. 3 (g) would be set to 1 (white). The features to be extracted are listed below.

- 1) Area: defined as the total pixels of the component and an area too small is considered as noise. Establishment of the standard depends on the demand of the industry. Here in this research the standard is set to 8 pixels.
- 2) Average gray value: defined as the mean of gray values retrieved from pixels of the component, and a pixel too bright is considered as a defect.
- 3) Eccentricity: to begin with, find out an ellipse owning the same second moments as the component. Furthermore, calculate the ratio of its focal length and major axis. An ellipse may also be defined as a perfect circle in which the eccentricity is 0; in a line the eccentricity is 1.
- 4) Ellipticity: to begin with, find out an ellipse owning the same second moments as the component. Furthermore, calculate the ratio of its major axis and minor axis. An ellipse is closer to a perfect circle as its ellipticity is closer to 1.

Toward each binary large object, there are two steps in the process of determining whether a defect exists or not. First and foremost, a component is viewed as a candidate circular pattern of which the eccentricity and ellipticity are both under the threshold. Moreover, a component is considered defective if the gray value of the candidate circular pattern is too high. Otherwise it is viewed as a circular pattern. Additionally, a component is considered defective unless the area of the circular pattern is small enough to be neglected.

III. EXPERIMENTS AND RESULTS

In this section, training of the parameters associated with the proposed defect inspection algorithm is discussed before the results of the inspection are displayed.

A. Parameter Sensitivity Experiment

Several parameters within the defect inspection algorithm need to be tested and decided through experimentation. Therefore this research chooses 20 flawless and flaw samples for the training.

1. Domain of Vector Valued Features of the Circular Pattern in Defect-Identifying Sub Function

To prevent the algorithm from making erroneous decisions that some circular pattern on the molding is defective, the research tries to distinguish it from a defect in terms of average gray value, eccentricity and ellipticity. Specific procedures start by circling manually all of the circular patterns pertaining to the flawless training samples. Then extract their features

respectively. We add standard deviations to the mean of each feature, and the multiple should be an integer dependent on the maximum value. Fig. 4 exhibits the distribution of average gray value, eccentricity and ellipticity of circles in the training samples. As a result, the threshold of each feature may be calculated, in which the upper limit of the average gray value is 125.4; the upper limit of the eccentricity is 0.274; the upper limit of the ellipticity is 1.041.

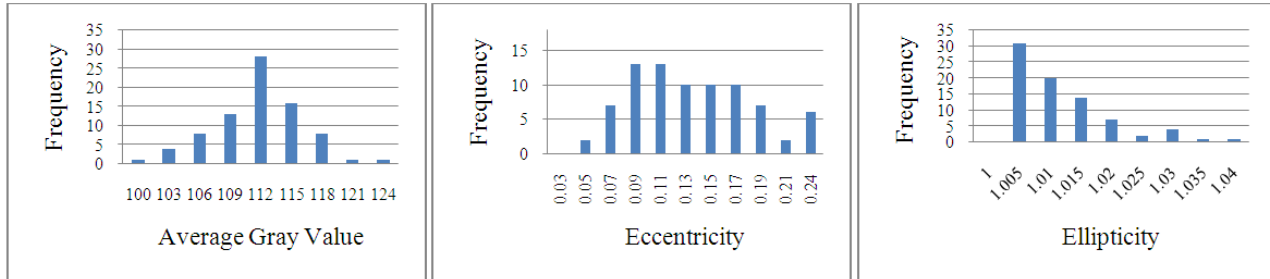


Fig. 4 Distribution of each feature

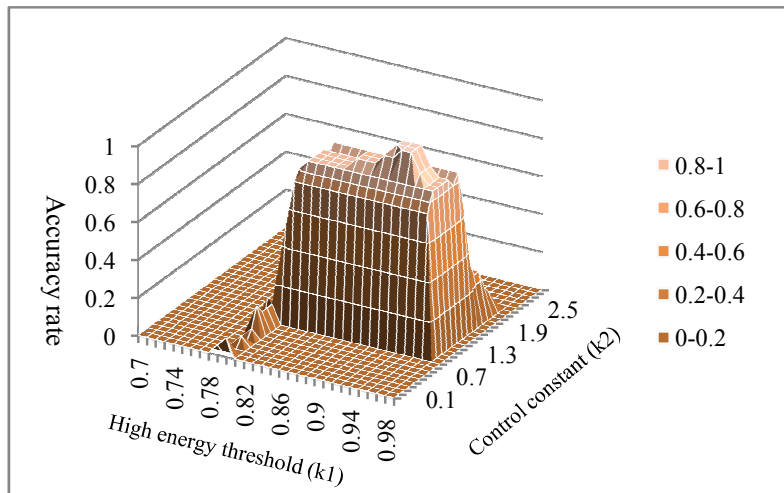


Fig. 5 Accuracy rate of inspection measured with different combinations of k_1 and k_2

2. High Energy Threshold and Control Constant in the Sub Function of DFT-Based Image Restoration Scheme

The parameter configuration of the features stated above would be feasible provided a proper high energy threshold (k_1) and control constant (k_2) could be figured out. The k_1 is the control parameter manifested by (3) to generate the notch-rejected filter. Once the k_1 is too small, redundant filters may filter out the defects, textures and circular patterns en masse. Yet if the k_1 is too big, only a few filters are located at the center of the image in the frequency domain; consequently, the textures cannot be excluded effectively. And the k_2 introduced by (5) is the parameter controlling the UCL, differing the texture from defects and circles during the image restoration process. Once the k_2 is too small, the control limit would be very tight, and it would be more difficult to completely eliminate the textures. Accordingly too much noise

would be disclosed by a binary image. On the other hand, a too big k_2 means a much slacker control limit; in consequence the texture, defects and circles may partly or wholly be disposed of. For the sake of credible k_1 and k_2 , this research uses various combinations of the parameter ($k_1=0.7, 0.71, \dots, 1.0; k_2=0.1, 0.2, \dots, 3.0$) to carry out defect inspection algorithm upon the training samples, and then logs the accuracy rate under each circumstance. In Fig. 6, we can see the peaks, the accuracy rate of the inspection, when k_1 is configured between 0.91 and 0.95, combined with k_2 being set between 1.3 and 1.5. The other combinations derive more false alarms or frequent omissions of the detection.

B. Results of the Experiment

To perform the inspection capacity of the proposed defect inspection algorithm, the researchers select 64 inspection samples for verification, during which each parameter of the

algorithm is in accordance with the recommended values or the median of recommended range of values determined by the last section. The result shows that the accuracy rate reaches 93.75%, with 6.25% omission of the detection. From Figs. 6(a1) to 6(a6), images of molding surfaces are presented before

the algorithm is carried out, followed by binary images, as shown from Figs. 6(b1) to 6(b6). A flawless image is fed back with a white clean picture as a response. In addition, the feedback of a defective image is a picture pointing out thorough shape and location of the imperfection.

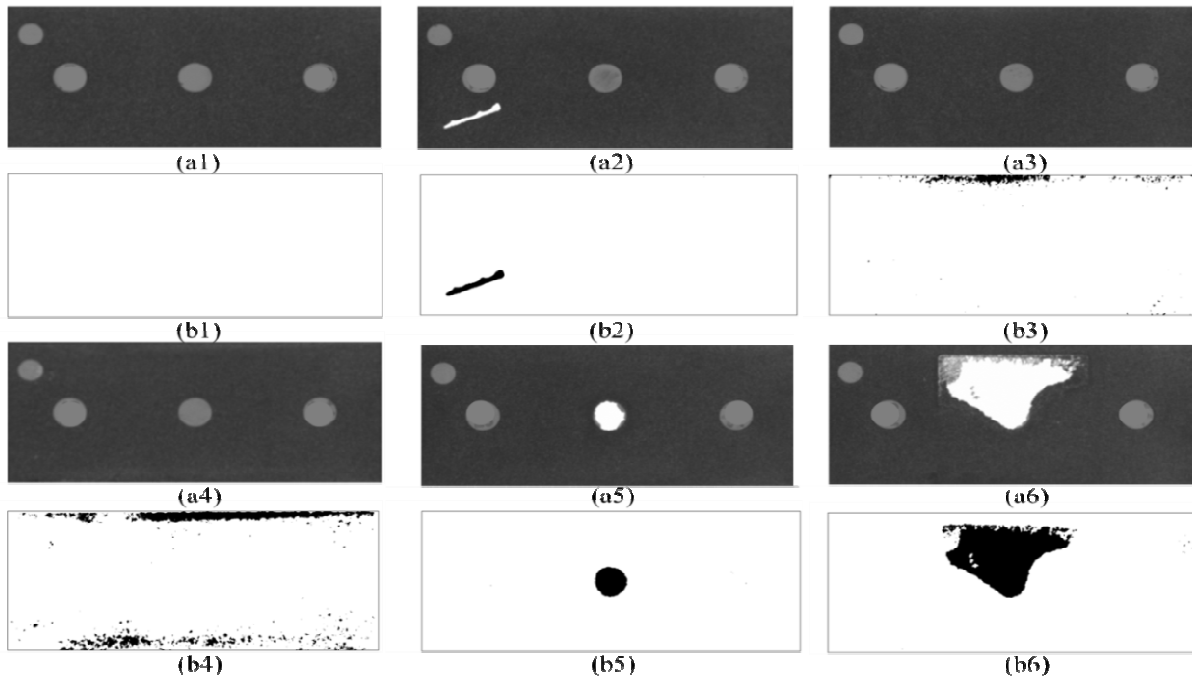


Fig. 6 Results of experiment: (a1) flawless molding surface; (a2) molding surface with cracks; (a3)-(a4) molding surface with voids; (a5)-(a6) molding surface with dilapidation; (b1)-(b6) corresponding binary images

IV. CONCLUSIONS

The research proposed a set of automatic optical inspection system for IC molding surface. First of all, the system automatically snatched images of a molding surface. Then the captured images were normalized, shrunk and segmented by way of the proposed sub functions automatically and the to-be-inspected blocks were attained. Next, random textures of the molding surface were removed by discrete Fourier-based image restoration scheme, though the cracks, voids and dilapidation were kept. The inspection system works effectively with high accuracy rate of 93.75%.

ACKNOWLEDGMENT

This research is partially supported by the National Science Council, Taiwan, under contract no. NSC 02-2218-E-131-002.

REFERENCES

- [1] P.Yalamanchili, A.Christou, S.Martell, and C.Rust, "CSAM sounds the warning for IC packaging defects," *IEEE Circuits Devices Mag.*, vol. 10, no. 4, 1994, pp. 36-41.
- [2] S.H.Ong, S.H.Tan, and K.T.Tan, "Acoustic microscopy reveals IC packaging hidden defects," *Proc. 1997 1st Electronic Packaging Tech. Conf.*, 1997, pp. 297-303.
- [3] L.Ma, S.Bao, D.Lv, Z.Du, and S.Li, "Application of C-mode scanning acoustic microscopy in packaging," *8th Int. Conf. Electronic Packaging Tech.*, 2007, pp. 1-6.

- [4] D.M.Tsai, and T.Y.Huang, "Automated surface inspection for statistical textures," *Image Vision Comput.*, vol. 21, no. 4, 2003, pp. 307-323.
- [5] D.B.Perng, S.H.Chen, and Y.S.Chang, "A novel internal thread defect auto-inspection system," *Int. J. Adv. Manuf. Tech.*, vol. 47, no. 5-8, 2010, pp. 731-743.

Ssu-Han Chen is an assistant professor in the Department of Industrial Engineering and Management in Ming Chi University of Technology, New Taipei City, Taiwan. He received his Ph. D. degree in Industrial Engineering and Management from National Chiao Tung University (NCTU), Taiwan, in 2010. His current research interests include digital image processing, machine vision, pattern recognition, patentometrics, and social network analysis.

Der-Baau Perng is a distinguished professor in the Department of Applied Informatics and Multimedia, Department of International Business in Asia University, Taichung, Taiwan. He received his Ph. D. degree in Computer Engineering from National Chiao Tung University (NCTU), Taiwan, in 1988. He was the Chairman of the Department (1991-1994, 2006-2009), the Director of Production System Automation Research Center (1995-1996), the Executive Manager of NCTU Spring Foundation (1998-1999), the Director of Alumni Communication Center (1998-2000), the Director of Semiconductor Manufacturing Management Center (1997-2001), the Secretary-in-chief of NCTU (2003-2007), the Dean of Management College in Yu Da University of Science and Technology (2011-2012), and the Distinguished Professor in Asia University (2012-present). His current research interests include computer vision, CAD/CAM integration, e-commerce, and supply chain management.